Construction and Building Materials 418 (2024) 135400

Contents lists available at ScienceDirect

Construction and Building Materials

journal homepage: www.elsevier.com/locate/conbuildmat

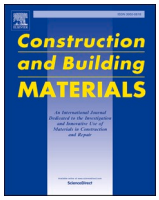

Study of the correlation of the mechanical resistance properties of Macael white marble using destructive and non-destructive techniques

Ma Paz Sáez-Pérez [a,*,1], Jorge A. Durán-Suárez [b,2], Joao Castro-Gomes [c,3]

[a] Building Constructions Department, Advanced Technical School for Building Engineering, University of Granada, Campus Fuentenueva, C/ Severo Ochoa, s/n -18071 Granada, Spain
[b] Department of Sculpture, Faculty of Fine Arts, University of Granada, Andalucía s/n. Edif. Aynadamar, 18071 Granada, Spain
[c] Department de Engenharia Civil e Arquitectura, University of Beira Interior, Calçada Fonte do Lameiro, 6201-001 Covilhã, Portugal

ARTICLE INFO

Keywords:
Thermal gradient
Correlation
Macael marble
Mechanical properties
Non-destructive testing
Accelerated testing
Built heritage

ABSTRACT

The current research explores the influence of thermal gradients on the mechanical strength of Macael marble using both Non-Destructive Testing (NDT) and Destructive Testing (DT). The material undergoes various temperature gradients (−20 and 300ºC) in sets of daily accelerated aging cycles (100 cycles). The results illustrate the impact of thermal gradients and reveal a decrease in the material's mechanical properties of up to 24%. Moreover, the reduction observed in the initial cycles at lower gradients (50 cycles, −20/50ºC) continues to progress with the increasing intensity and number of cycles. Changes induced in the microstructure manifest as microcracks between calcite grains. The correlation coefficient R2 > 0.9 confirms the effectiveness of non-destructive tests as reliable techniques for assessing the material's strength capacity and potential deterioration.

1. Introduction

In recent decades, there has been increasing interest in research into the conservation of both historical and modern buildings with artistic and heritage value [1]. Architectural heritage, as part of our cultural heritage, plays a crucial role in the creation of new spaces and the development of our cities.

At the same time, one of the critical challenges facing the world today is sustainable development and how best to achieve it. This has important implications in all fields and heritage conservation is no exception. This has led to demands for a new approach that combines both protective and conservation work [2–4], recognizing the diverse heritage values attributed to buildings [5–8] and thus helping to protect the environment and promote the sustainability of our cities [9,10]. Within this context, it is essential to ensure the conservation and promotion of cultural heritage. This will have an immediate impact on achieving the Sustainable Development Goals (SDGs), as a cross-cutting promoter of those relating to the safety and sustainability of urban areas, the slowdown of environmental degradation, sustainable and clean energy, and the fostering of partnerships to achieve these goals [11], all of which contribute to promoting peaceful and inclusive societies [12]. In line with this approach, the European Union has set itself a strategic goal for the 21st century to achieve the sustainability and renewal of architectural heritage buildings [13].

In recent times, the proper conservation of built heritage has become essential for its use and enjoyment, and for the creation of tourist attractions, leading to a significant increase in its importance and its influence within society [14,15]. The preservation of architectural heritage now plays a crucial role in enhancing the quality of life of the residents of our towns and cities and also makes an important contribution to the local economy and cultural life [14,15].

However, ensuring the preservation and restoration of heritage buildings involves adapting them to new uses and conditions, complying with new regulations, and addressing the issues arising from outdated historic construction systems, so as to prevent damage and environmental impacts that could jeopardize their survival. These buildings must be conserved without altering their original character [16–18] and to this end action must be taken to prevent deterioration and control ageing processes [19,20].

Successful heritage intervention work requires specific knowledge

* Corresponding author.
E-mail address: mpsaez@ugr.es (M.P. Sáez-Pérez).
[1] orcid.org/0000-0001-9725-1153
[2] orcid.org/0000-0002-9714-3555
[3] https://orcid.org/0000-0002-2694-5462.

https://doi.org/10.1016/j.conbuildmat.2024.135400
Received 10 August 2023; Received in revised form 23 December 2023; Accepted 7 February 2024
Available online 13 February 2024
0950-0618/© 2024 The Author(s). Published by Elsevier Ltd. This is an open access article under the CC BY-NC-ND license (http://creativecommons.org/licenses/by-nc-nd/4.0/).

about the buildings and the necessary techniques for studying and evaluating the state of the building and the work that may be required. Historical studies must be combined with the characterization of the building materials, assessing their nature, properties, the state of degradation, environmental conditions, stress levels, and their possible evolution. To this end, a wide range of experimental techniques can be applied, often involving sampling. However, due to their enormous cultural value, only a limited number of samples may be taken from heritage buildings, so making non-destructive testing (NDT) essential, and sometimes the only way to analyze them. In order to preserve these objects in the most intact form possible, the use of NDT has become imperative, even during restoration itself. NDT methods can be used to assess the effectiveness of improvements and compliance with building and other regulations [21,22]. However, the fact that only a very limited number of destructive tests can be performed makes their results less representative or reliable. These results must therefore be verified and validated with other tests that can assess the state of the materials within the shortest feasible timeframe [23]. Over the years, researchers have sought to improve NDT techniques for diagnostic and monitoring purposes, with a view to achieving more reliable, more accurate results. This often involves combining several different techniques [24]. Various researchers have investigated this question, highlighting the importance of NDT in the study of built heritage [4,25–29].

As regards the types of damage most commonly evaluated using NDT, these include those with a significant impact on the structural and hygrothermal behavior of the buildings, such as defects and cracks, often exacerbated by adverse humidity and temperature conditions. These kinds of damage in building materials can be identified via the changes observed in their physical properties [30].

When studying built heritage, the best solution is a combination of correlated NDT techniques, and numerous research projects have been conducted into the different building materials, often with specific case studies [31–33]. These studies involve many different properties of the building materials and are becoming increasingly common [34,35].

According to the literature [36], ultrasonic testing and Schmidt Hammer rebound hardness are the most common NDT techniques used for the study and analysis of the structural behavior of building materials, due to their simple application and low cost. These tests can detect variations in the original properties of the building materials, clear evidence of decay or defects.

The behavior of natural materials such as marble depends to a large extent on their formation conditions, such as composition, mineralogical and petrological arrangement, and anisotropy [37]. The environmental conditions to which the materials are exposed in the quarry and subsequently during their use in a building can lead to alterations of different kinds. When planning the structural, construction, energy, and aesthetic aspects of any restoration project, it is therefore essential to understand the evolution and the behavior of the material once in use in the building.

In the case of Macael marble, previous studies [38–43] provide significant results regarding the impact of thermal gradients on the material's behavior. Accelerated ageing tests have provided insights into the impact of changing conditions on marble [44–47], leading to improvements in design regulations [48] and serving as an effective method for studying its behavior [49].

Various publications [50–54] confirm that calcite crystals generally show anisotropic behavior from a thermal perspective. As temperature increases, the crystals expand parallel to the c-axis and contract perpendicular to it. This results in the opening of grain boundaries. Prolonged exposure to high temperatures leads to increased expansion effects, making the material more sensitive to environmental conditions. This behavior is considered the primary cause of marble deterioration, and studies are required to determine the level of damage and the impairment of its properties so as to facilitate decision-making for possible repair or restoration work.

Based on the previous background, this research aims to assess the impact of ageing cycles on material behavior and, and on the other hand to determine the effectiveness of non-destructive tests in establishing the load-bearing capacity of Macael marble by correlating the results. In order to ensure the reliability of non-destructive tests as valid methods for assessing load-bearing capacity, the investigation involves analyzing the stone material under both natural conditions and accelerated ageing. This comprehensive analysis enables the prediction of the material's capacity in various states of deterioration.

The methodological approach developed has focused on conducting various tests to determine the load-bearing capacity for the different considered ageing phases. This approach has allowed us to determine whether the incidence of temperature ranges occurs at low or high temperatures, as well as to establish the level of correlation between the two types of techniques (NDT and DT), which have not been evaluated for this material until now, constituting the main novelty of the study. The results will facilitate the assessment of conservative interventions that may be proposed as part of strategic planning at the monument scale, allowing actions related to evaluation, management, protection, and sustainable development applied to built cultural heritage.

Fig. 1 shows the flowchart corresponding to the conducted research.

Finally, it is worth noting that the proposed research could be applied to other types of building materials subjected to different alteration conditions, offering the possibility of understanding their condition before restoration interventions. In such cases, the conditions that best suit their situation would need to be established to propose the temperature range and the number of cycles.

2. Materials and methods

2.1. Materials

The decision to focus on the study of Macael marble in this research is driven by its significance in the context of universal heritage and its susceptibility to deterioration from environmental exposure. Understanding its evolution and characteristics through studies is paramount.

The term "White Macael" encompasses various commercial varieties depending on the extraction area and the trading company [55]. The white lithotype is extensively used in historical architecture and sculpture within the Spanish built heritage. Similar lithotypes can be identified in numerous world heritage sites, spanning both ancient and recent periods. Examples of global renown include the Alhambra in Granada and other palaces such as the Roman Theatre in Mérida (1st century BCE), Phoenician anthropomorphic sarcophagi in Gadir-Cádiz (5th century BCE), Alcazaba of Almería (11th century), Medina Azahara Palace in Córdoba (10th century), and the Monastery of San Lorenzo de El Escorial (16th century) in Spain. Noteworthy instances from the 20th century include the Metropolitan Museum of Art in New York (1913) and the Burj Al Arab building in Dubai (1994). In recent years, White Macael marble has achieved international prominence on all five continents, with a notable presence in the United States, Asia, and the United Arab Emirates.

Geologically, Macael marble belongs to the Nevado-Filabride complex. This complex is situated in the lower regions of the Betic mountain range, specifically known as the Internal Zones [56]. From a tectonic perspective, the Nevado-Filábride complex can be further categorized into upper and lower zones [57], with the Macael quarries positioned in the upper part. The complex was formed through low thermal gradient and high-pressure metamorphosis, succeeded by other thermal gradients with higher temperatures [55]. The materials constituting this complex date back to a period ranging from the Precambrian to the Jurassic.

Regarding the era of metamorphism, it appears to have occurred primarily during the Alpine orogeny (Upper Cretaceous-Miocene) [58]. The resultant material comprises carbonated rocks from the Upper Triassic age, interspersed with various types of mica schists, including calcareous, quartzitic, garnet-bearing quartzitic mica schists, and

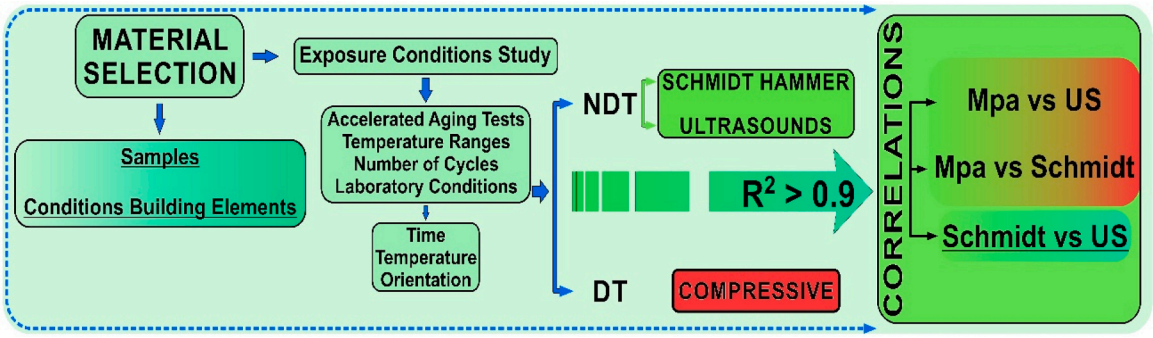

Fig. 1. Flowchart showing the main dataset, processing steps and analyses in this study.

amphibole-bearing quartzitic mica schists.

As regards the Macael marble used in this research, a selection of test specimens can be seen in Fig. 2. It typically exhibits alternating white and (more or less visible) gray stripes, with a preferential direction in the blocks extracted from the quarry.

In a prior study [47], the marble samples investigated in their natural state were characterized based on their petrographic features and mineralogical composition, as outlined below. Fig. 3 illustrates the X-ray diffraction (XRD) analyses conducted on two samples, and Table 1 provides the results of the X-ray fluorescence (XRF) test on four samples [59].

The average grain size of the marble falls within the range of 0.16 to 3.2 mm. Visually, it exhibits a homogeneous morphology with a mosaic-like texture, displaying granoblastic characteristics that vary from equigranular to heterogranular. The grains show a range in size from large to medium-fine. Mineralogical characterization tests conducted in a previous study [59] affirm that Macael marble is predominantly composed of calcite, with small amounts of quartz, along with isolated muscovite and feldspar crystals. Of note are the physical properties, which include open porosity values ranging from 0.1% to 0.6%, and apparent density values spanning from 2.50 to 2.75 g/cm^3 .

In the current research, prior to conducting the tests and in adherence to applicable regulations, the marble samples were cut into prisms measuring 15×5x5 cm.

3. Methodology

3.1. Accelerated ageing test - artificial weathering

In this case, aiming to understand the alteration process of Macael marble in detail, and based on previous studies [52,53,61], the selection of accelerated ageing test conditions is determined after recognizing the exposure conditions in its context, for that reason, the standard method is not applied. This type of material is subjected to temperature conditions that experience significant daily changes and high thermal gradients [59,61]. In the research phase, these variations are replicated through cycles in accelerated test conditions. The evaluation of the effects produced on the material, using a combination of wide-ranging thermal gradients, is proposed in this study, under higher thermal conditions than those used in previous research.

For this purpose, each combined cycle (heating-cooling-freezing) is considered to represent a daily cycle (24 h), simulating various stages of thermal exposure that involve a significant thermal contrast equivalent to atmospheric conditions outdoors (temperatures above and below 0ºC). The study amplifies the maximum and minimum temperatures in the daily cycles to achieve a more immediate effect. Simultaneously, there is a proposal to increase the number of cycles conducted thus far, allowing for the prediction of real effects on the material in a shorter period.

The thermal gradients were categorized into temperature ranges between − 20ºC and 300ºC. In total, seven groups of marble samples (refer to Table 2) were subjected to different conditions (one control

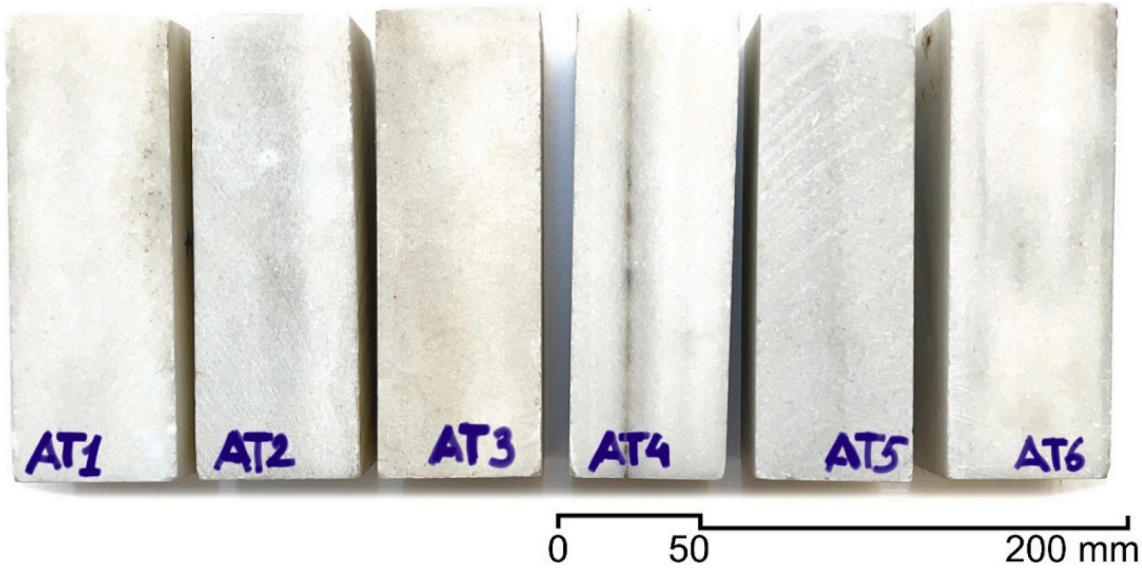

Fig. 2. Selection of samples tested in this research study, indicating their nomenclature.

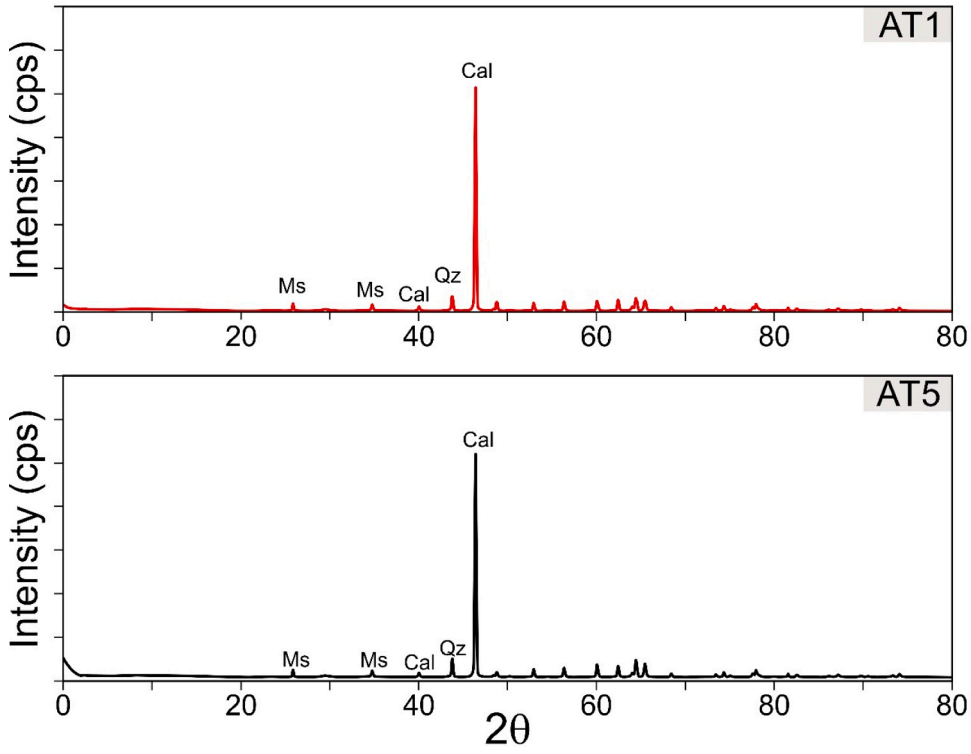

Fig. 3. X-ray diffractograms for the samples of Macael marble (Almería, Spain) studied in this research work. The mineralogical results were identical for all the lithotypes analyzed (AT1 and AT5). Abbreviations for the names of rock-forming minerals [605]. Legend: Cal = calcite; Ms = muscovite; Qz = quartz.

Table 1
Chemical composition by XRF analysis (wt%) of the Macael marble (Almería, Spain) samples studied in this research work. Data are normalized to 100% (LOI-free).

CaO	SiO2	Al2O3	MgO	Na2O	K2O	Fe2O3	TiO2	P2O3	LOI
55,00	0,36	0,04	1,32	0,06	< 0,01	0,13	0,01	0,05	43,03
55,20	0,36	0,01	1,42	0,07	< 0,01	0,04	0,01	0,06	42,83
54,70	0,42	0,04	1,33	0,06	< 0,01	0,04	0,01	0,07	43,33
55,30	0,21	< 0,01	1,27	0,07	< 0,01	0,03	0,01	0,04	43,07

Table 2
Work Plan and Name of Sample Groups, Number of Cycles, and Environmental Conditions for Accelerated Ageing Tests (Heating, Cooling, and Freezing).

Sample groups	Number of 24-hour cycles	Maximum temperature/hours	Minimum temperature/hours
AT0	0	Room temperature (22ºC±1ºC, RH=37% ±5%	Room temperature (22ºC ± 1ºC, RH=37% ± 5%
AT1	100	50ºC/10 h	-20ºC/ 10 h
AT2	100	100ºC/10 h	-20ºC/ 10 h
AT3	100	150ºC/10 h	-20ºC/ 10 h
AT4	100	200ºC/10 h	-20ºC/ 10 h
AT5	100	250ºC/10 h	-20ºC/ 10 h
AT6	100	300ºC/10 h	-20ºC/ 10 h

Of the 4 remaining hours to complete the 24-hour daily cycle, 2 h were devoted to the transition from maximum to minimum temperature and a further 2 h to the transition from minimum to maximum

group that received no treatment and six groups subjected to 100 cycles of various thermal gradients). Controls, employing different techniques (DT and NDT), were conducted every 25 cycles. The thermal gradient cycle to which each group is subjected is illustrated in Fig. 4.

In all cases, including the control group, 20 specimens per group were tested, resulting in a total of 140 specimens. The rebound value, ultrasonic pulse velocity, and mechanical strength until failure were measured in the direction of greatest significance for the specimen (direction z or height), aligning with the direction of the maximum load in which the material is placed.

The heating/cooling cycles were conducted by placing the specimens in a convection heating oven and a freezer, respectively. A GGM Gastro International GmbH model SKU TC2126 freezer was utilized for the freezing cycle, and a HAIDA EQUIPMENT HD-E804 convection oven was employed for the heating test.

Simultaneous testing of the specimens was carried out to ensure uniform exposure to the same laboratory conditions, maintaining a temperature of 22ºC ± 1ºC and a relative humidity of HR= 37 ± 5%.

3.2. Schmidt hammer

A Schmidt Rebound Hammer (Rock Schmidt RS8000 model), recommended for rock testing, was employed for the rebound index test. Six rebounds were performed on each specimen, perpendicular to the measuring plane and at a distance of > 10 mm from the edge.

Twenty samples were tested in each group (AT0-AT6), corresponding to four samples in each batch of cycles (0, 25, 50, 75, and 100 cycles). The data for each specimen were obtained from the arithmetic mean of all the measurements taken for each specimen, after eliminating any anomalous data. The test was conducted following the recommendations of [63].

Prior to the test, it was ensured that the surfaces of the specimens were smooth, clean, and dry.

Measurements were taken on the untreated control samples and after

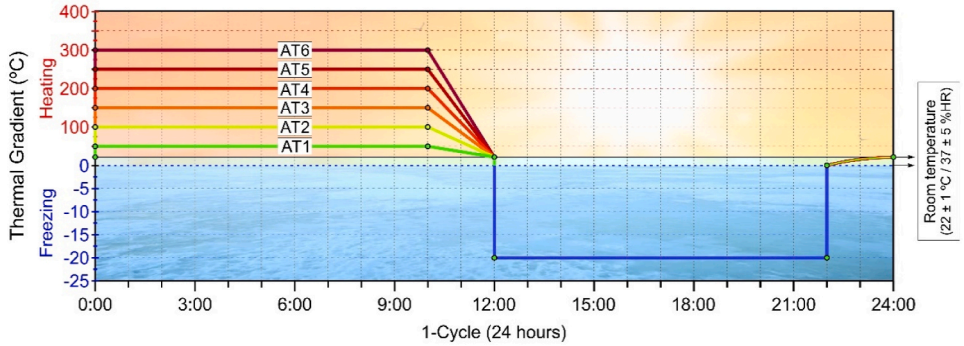

Fig. 4. Model of the heating, cooling, and freezing cycle used in this study as an accelerated ageing test on various groups of Macael marble samples (Almería, Spain). Note that one complete cycle lasts for 24 h.

each batch of heating/cooling cycles described. Each measurement was repeated three times to ensure the reproducibility of the test and the reliability of the results.

3.3. Ultrasonic pulse velocity test

Ultrasonic pulse velocity was measured using the direct transmission method. Two sensors were placed at each end of the specimen under constant pressure, with one acting as the transmitter and the other as the receiver. To ensure proper coupling between the specimen and the transducers, a viscous crystal ecogel, Quick Eco brand, was utilized.

The ultrasonic equipment comprised a STEINKAMP BP V with a low-power pulse generator and high-power emission and reception transducers capable of generating pulses of 50 and 100 KHz. Given the material and the size of the blocks, waves with a frequency of 100 KHz were employed. The test followed the recommendations of [64].

Vp was calculated according to the following formula:

$$Vp = L/t$$

where L is the length of the sample (distance between transducers), measured in meters, and t is the average transit time of the ultrasonic signal, measured in seconds, for each of the three measurements taken at the same location.

As with the rebound test, the test was conducted on untreated material and after each batch of heating/cooling cycles. tested 20 samples in each group (AT0-AT6), corresponding with 4 samples in each batch of cycles (0, 25, 50,75 and 100 cycles).

3.4. Compressive strength

For the compressive strength test, an Ibertest Eurotest MD2 universal testing machine was employed. This equipment allows for varying load characteristics from 2 kN to 2000 kN and maintains a continuous record of the stress (MPa) and deformation (mm/m) in the sample block until failure. The load application speed during the test was 5 mm/min. Twenty samples in each group (AT0-AT6) were tested, corresponding to four samples in each batch of cycles (0, 25, 50, 75, and 100 cycles). Results were obtained for each specimen tested in the different groups. The test was conducted following the recommendations of [65]. The dimensions of the marble samples were 15×5x5 cm.

3.5. Optical microscopy and SEM

The changes induced in the microstructure of the samples after the thermal cycles were investigated using thin sections with a polarized optical microscope (Olympus BX-60). For the SEM study, a Zeiss DMS 950 scanning electron microscope (SEM) coupled with Microanalysis Link QX 2000 was used.

4. Results

4.1. Non-destructive tests

The rebound values and ultrasonic pulse velocities for the different groups of specimens are presented in Tables 3 and 4 and Figs. 5 and 6.

5. For enhanced readability, the percentage loss values in the tables and comments have been rounded to whole numbers

5.1. Schmidt hammer rebound

Table 3 presents the results for each group at different control points (after 25, 50, 75, and 100 cycles).

In this test, the results indicate a consistent decrease in the rebound value across all groups, with variations based on the number of cycles and the conditions to which the samples were exposed in the accelerated ageing test. Following the initial 25 cycles, there was a decrease ranging from 18% for specimens subjected to cycles 50/− 20ºC (AT1) to 39% for those exposed to 300/− 20ºC (AT6). Group AT3, subjected to 200/− 20ºC, exhibited an intermediate value of 29%.

The reduction in the rebound values was confirmed for all the groups, although it varied according to the type of ageing conditions applied.

If the behavior at different stages of the ageing process is analyzed, the results indicate a significant loss in rebound values during the first 25 cycles, with a maximum difference of 39% observed in group AT6. In the next stage between 25–50 cycles, a maximum reduction of 16% could be observed in groups AT2 and AT3. In the third and fourth stages (between 50–75 and 75–100 cycles), there were much smaller reductions with a maximum difference of 4.3% in the last control and very similar values in all the groups.

The results are presented in Fig. 5, highlighting the decrease in the rebound value in line with the increase in the number of cycles and the ageing conditions in each group of specimens. It also shows that the impact on the rebound value is not as pronounced once the 50 cycles' mark has been passed. This indicates that the ageing process affects the properties of the marble from the early stages of the test, and that these effects become less intense as the number of cycles increases.

5.2. Ultrasonic pulse velocity

In the results of the ultrasonic pulse velocity test, a similar reduction in values, as observed in the previous test, is evident. Similarly, this reduction is more significant in the controls conducted after 25 and 50 cycles for the different groups. Across all groups, the results indicate a significant decrease in ultrasonic pulse velocity values as the number of cycles increases. Reductions of 42% are observed for group AT1, subjected to milder ageing conditions, and 47% for group AT6, exposed to

Table 3
Rebound value, standard deviation, and percentage loss in the sample groups after 25, 50, 75, and 100 cycles.

GROUP	0 cycles	25 cycles	Lost (%)	50 cycles	Lost (%)	75 cycles	Lost (%)	100 cycles	Lost (%)
AT1	36.00 ± 0.90	29.52 ± 5.48	18%	24.12 ± 3.11	34%	22.32 ± 1.07	39%	20.88 ± 2.46	44%
AT2	35.94 ± 1.20	27.67 ± 2.26	23%	22.47 ± 4.37	39%	21.64 ± 6.14	41%	19.77 ± 2.30	45%
AT3	36.17 ± 0.18	25.68 ± 1.23	29%	22.20 ± 3.20	40%	20.98 ± 1.35	43%	19.89 ± 2.29	47%
AT4	36.44 ± 1.03	24.05 ± 7.41	34%	22.04 ± 3.19	41%	20.84 ± 1.42	43%	19.78 ± 5.13	47%
AT5	36.44 ± 0.75	22.59 ± 1.33	38%	21.03 ± 2.41	42%	20.65 ± 1.01	43%	19.53 ± 1.14	47%
AT6	36.73 ± 0.45	22.41 ± 2.21	39%	20.99 ± 1.03	43%	20.20 ± 3.36	45%	19.46 ± 2.22	48%

Legend: AT1 (50/−20ºC); AT2 (100/−20ºC); AT3 (150/−20ºC); AT4 (200/−20ºC); AT5 (250/−20ºC); AT6 (300/−20ºC)

Table 4
Mean values for ultrasonic pulse velocity (m/s), standard deviation, and percentage loss in the sample groups after 25, 50, 75, and 100 cycles.

GROUP	0 cycles	25 cycles	Lost (%)	50 cycles	Lost (%)	75 cycles	Lost (%)	100 cycles	Lost (%)
AT1	5695.00 ± 50.22	5011.60 ± 200	12%	3815.65 ± 180.44	33%	3530.90 ± 260.18	38%	3303.10 ± 170.34	42%
AT2	5581.00 ± 21.84	4576.42 ± 130	18%	3489.80 ± 90.31	37%	3359.76 ± 170.36	40%	3069.55 ± 140.28	45%
AT3	5644.00 ± 30.21	4233.00 ± 60	25%	3463.72 ± 140.40	39%	3273.52 ± 210.42	42%	3104.20 ± 80.17	45%
AT4	5679.00 ± 21.10	3918.51 ± 100	31%	3435.23 ± 110.20	40%	3248.39 ± 150.15	43%	3081.99 ± 90.46	46%
AT5	5715.00 ± 10.22	3714.75 ± 160	35%	3297.56 ± 220.34	42%	3239.26 ± 80.22	43%	3063.24 ± 160.13	46%
AT6	5603.00 ± 40.81	3529.89 ± 120	37%	3202.11 ± 210.17	43%	3081.65 ± 60.21	45%	2969.03 ± 120.22	47%

Legend: AT1 (50/−20ºC); AT2 (100/−20ºC); AT3 (150/−20ºC); AT4 (200/−20ºC); AT5 (250/−20ºC); AT6 (300/−20ºC)

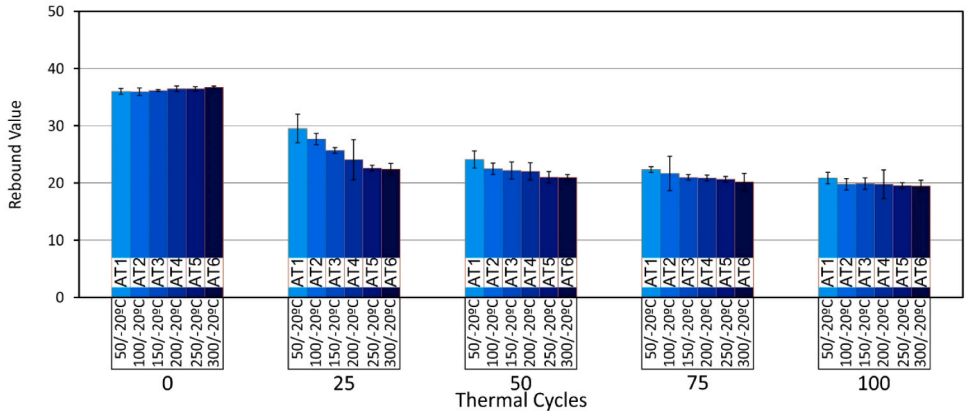

Fig. 5. Graphs displaying the results of the Schmidt hammer rebound test for the six groups of marble samples, categorized according to the ageing test conditions up to 100 cycles (AT1: "−20/50 °C; AT2: "−20/100 °C; AT3: "−20/150 °C; AT4: "−20/200 °C; AT5: "−20/250 °C; and AT6: "−20/300 °C). The graph illustrates both the mean values for each group and the resulting standard deviations.

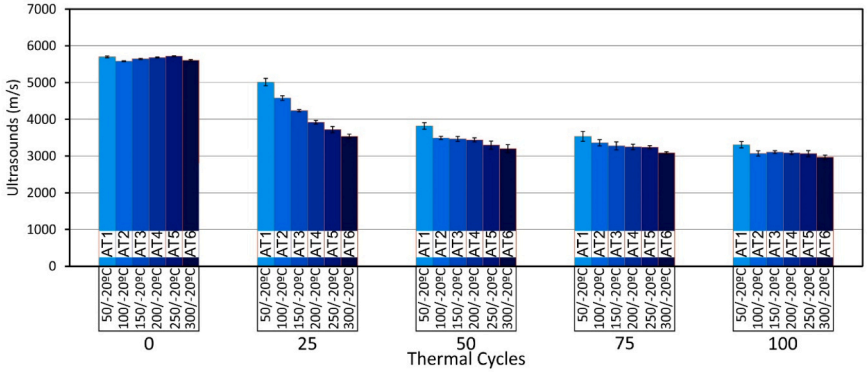

Fig. 6. Ultrasonic pulse velocity results for the six sample groups, classified according to the ageing test conditions up to 100 ageing cycles (AT1: "−20/50 °C; AT2: "−20/100 °C; AT3: "−20/150 °C; AT4: "−20/200 °C; AT5: "−20/250 °C; and AT6: "−20/300 °C). The graph displays both the mean values for each group and the resulting standard deviations.

more intense conditions.

Similar to the rebound test, the most significant impact occurred during the first two stages (0–25 and 25–50 cycles), with the maximum effect observed during the initial 25 cycles, resulting in reductions of up to 37% in group AT6. In Stage 2 (25–50 cycles), a greater reduction in velocity was noted for groups AT1 and AT2, with maximum values of 21% and 19.47%, respectively, while the reduction was less pronounced in the other groups with more intense ageing test conditions. In tests

conducted after 75 and 100 cycles, a continued decrease in ultrasonic velocity was observed, albeit to a lesser extent, with a maximum reduction of 5% and a minimum reduction of 2%.

As indicated by the obtained results, the reduction in velocity is consistent across all groups, being more pronounced in the initial stages and diminishing as the number of cycles advances.

Fig. 6 shows the UPV results on a graph, highlighting the decrease in velocity as the number of cycles advances in each group of specimens.

The values align with findings from comparable studies [47,52], confirming the reduction in ultrasonic velocity due to the various temperature gradients to which the samples are subjected and the number of cycles.

Upon examining the average ultrasonic velocity and rebound index values, it is observed that ultrasonic velocity values range from a maximum of 5581 m/s in the AT2 group after 0 cycles of accelerated ageing to the minimum value of 2969 m/s in the AT6 group after 100 cycles, representing a decrease of approximately 47%. Regarding the rebound index test, starting from a maximum value of 35.94 for AT2 with 0 cycles, it fell to a minimum value of 19.46 for AT6 with 100 cycles. This signifies that the maximum decrease was 48%, which is 1% more than the reduction obtained for the ultrasonic velocity test.

Comparing the results obtained in the non-destructive tests for the different groups, a similar trend is observed in all cases, with a reduction in values corresponding to the number of cycles and the intensity of the ageing tests specific to each group. This downward trend did not follow the same pattern in the two tests, as the percentage reduction in the ultrasonic velocity test was less intense in the initial cycles. However, in both cases, there was an evident decline in the values obtained, which was very similar for all the groups.

6. Compressive strength test

The results of the compressive strength test (a destructive test) are presented in Table 5 and Fig. 7.

Consistent with the non-destructive tests, a similar trend is evident. There is a noticeable reduction in the mechanical strength of the specimens in all the groups subjected to ageing cycles.

These cycles led to a maximum reduction in compressive strength of 15% for group AT1, 18% for group AT2, 20% for group AT3, and 22%, 23%, and 24% for groups AT4, AT5, and AT6, respectively.

In Fig. 7, the compressive strength results are presented in graph format, highlighting the trend described above.

When analysing the data for each 25-cycle stage, the most significant reduction occurs between 0 and 25 cycles. During the first 25 cycles, the reduction in resistance in the different groups ranged from 7% in group AT1 to 15% in group AT6. These reductions continue in the following stages but with smaller percentage increments (minimum of 2% and maximum of 5%). After all 100 cycles had been completed, the final reduction in compressive strength was about twice the reduction that occurred in the first 25 cycles with a final reduction of 15% for group AT1 and 24% for group AT6.

The results of all these different tests show a consistent trend for each group and number of cycles. However, a higher reduction was obtained in the non-destructive tests than in the destructive test.

Finally, upon comparing the results obtained in the different tests, it was confirmed that they all follow the same trend, with lower velocities, rebound values, and compressive strength as the number of cycles increased and the temperature conditions became more intense. These results align with previous research [53,59], with variations in the absolute values, which could be attributed to differences in the conditions applied in the accelerated ageing tests.

6.1. Optical Microscopy and SEM

Optical microscope and SEM images were captured for some of the specimens after exposure to different numbers of cycles, allowing for a visual study of the impact of the ageing test.

In Figs. 8 and 9, the effect of the accelerated ageing can be observed in the directional expansion of calcite grains. The grain boundaries behave like joints between the different materials, and the gaps between them widen when they are subjected to thermal stress. This increase in the distance between the grains was the only change observed in the state of the marble samples, even when subjected to more intense thermal gradients.

The samples depicted in Fig. 8 are thin sections of Macael marble (Almería, Spain) observed with a transmitted light petrographic optical microscope, using crossed polarizers and an analyzer. In panel A, a control sample that has not been subjected to thermal ageing is shown. The calcite grains exhibit a high degree of maturity, with parallel lines corresponding to crystallographic packets and no spaces between the grains. Similarly, no significant gaps can be observed between the contacts of the calcite grains, indicating that the marble stone is perfectly cohesive at a granular level.

Concerning the sample in panel B (50/−20 °C, 25 accelerated ageing cycles), although it appears similar to the control sample, it exhibits gaps between the grains ranging from 1.5 to 5 μm. In the remaining samples (panels C and D), there are larger spaces between the grains ranging from ≥ 5 to 20 μm, and even splits within individual grains. These observations are consequences of the thermal stress produced by 75 cycles with a thermal gradient of 150/− 20 °C for Sample C and 100 cycles of accelerated ageing with a thermal gradient of 250/− 20 °C for sample D.

The samples highlighted in Fig. 9 exhibit a very similar pattern to that observed with the optical microscope, with intra-granular separation becoming more prominent as the number of accelerated ageing cycles and their thermal gradient increase.

7. Results - correlation

7.1. Correlation between the different techniques and each thermal treatment

The correlation between each non-destructive test and the destructive test in each temperature batch is illustrated in the following figures (see Figs. 10, 11, and 12).

The results obtained from correlating Non-Destructive Testing (NDT) rebound values with Destructive Testing (DT) MPa values reveal heterogeneous outcomes, although all R2 data exceed 0.9. Notably, there are population differences within each of the correlated groups. Graphically, AT1 displays a highly optimal correlation, with its data population evenly distributed in the linear pattern. In comparison,

Table 5
Compressive strength (MPa), standard deviation, and percentage loss in the different sample groups after 25, 50, 75, and 100 cycles.

GROUP	0 cycles	25 cycles	Lost (%)	50 cycles	Lost (%)	75 cycles	Lost (%)	100 cycles	Lost (%)
AT1	68.67 ± 0.11	63.86 ± 0.73	7%	61.80 ± 0.09	10%	59.74 ± 0.28	135	58.37 ± 1.36	15%
AT2	67.82 ± 2.34	61.38 ± 1.01	9%	59.27 ± 2.17	13%	56.49 ± 1.63	17%	55.61 ± 0.98	18%
AT3	68.03 ± 3.27	60.00 ± 0.60	12%	58.44 ± 1.32	14%	55.85 ± 1.81	18%	54.42 ± 0.84	20%
AT4	69.47 ± 1.42	60.51 ± 1.52	13%	58.91 ± 0.70	15%	56.20 ± 0.34	19%	54.19 ± 1.02	22%
AT5	68.09 ± 5.10	58.90 ± 0.33	14%	56.51 ± 0.62	17%	53.79 ± 1.30	21%	52.43 ± 0.67	23%
AT6	68.11 ± 3.23	57.89 ± 0.22	15%	55.58 ± 1.07	18%	52.58 ± 0.69	23%	51.76 ± 0.45	24%

Legend: AT1 (50/−20ºC); AT2 (100/−20ºC); AT3 (150/−20ºC); AT4 (200/−20ºC); AT5 (250/−20ºC); AT6 (300/−20ºC)

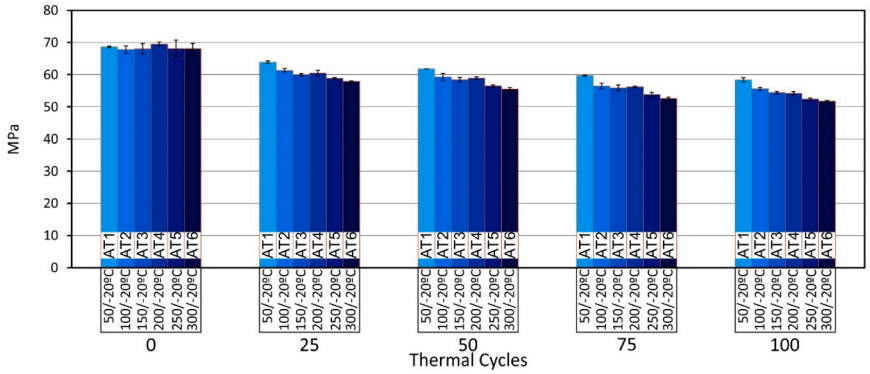

Fig. 7. Compressive strength results for the six sample groups, categorized according to the applied ageing test conditions up to 100 ageing cycles (AT1: "−20/50 °C; AT2: "−20/100 °C; AT3: "−20/150 °C; AT4: "−20/200 °C; AT5: "−20/250 °C; and AT6: "−20/300 °C). The graph displays both the mean values for each group and the resulting standard deviations.

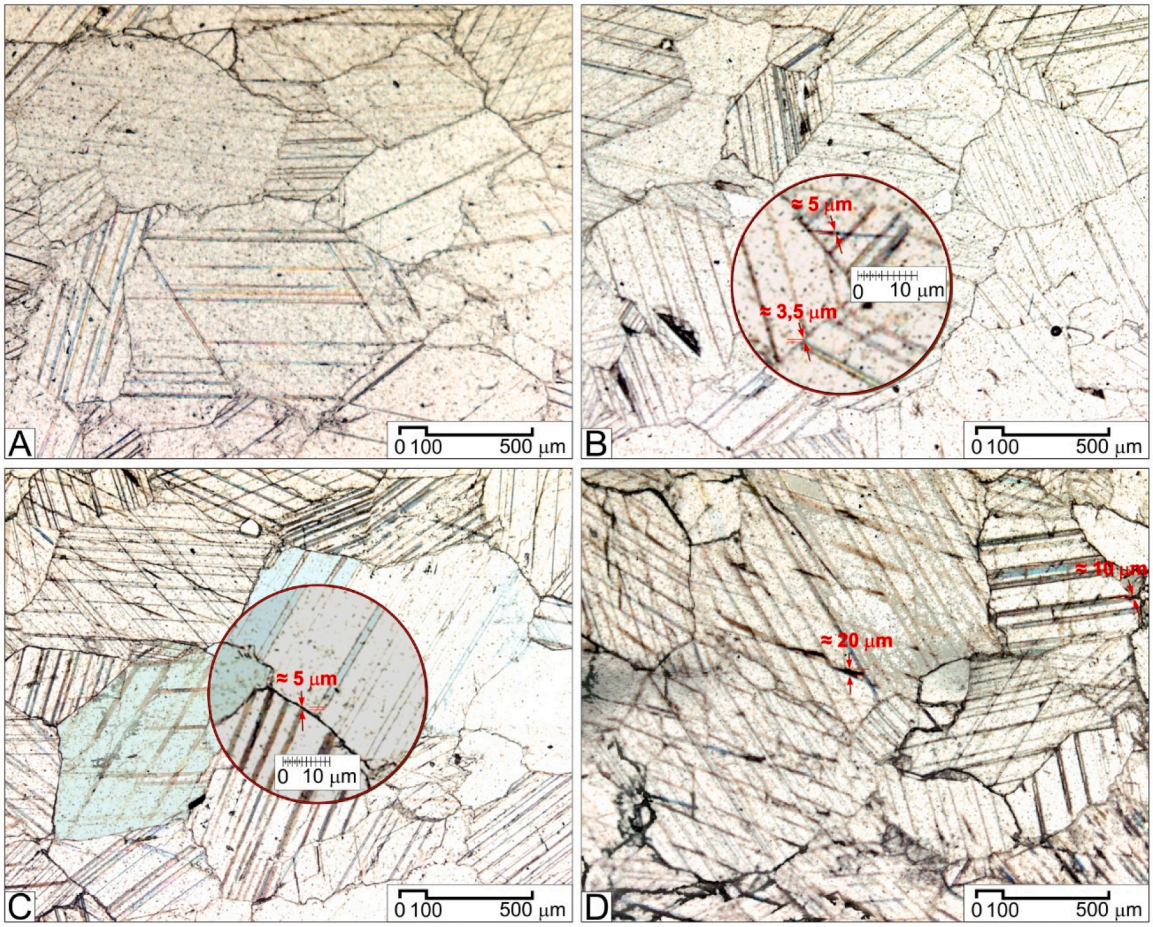

Fig. 8. Optical microscope (20x) images of unaltered and thermally altered samples of Macael marble. A. AT0 "0" cycles. B. AT1 "50/− 20ºC", 25 cycles. C. AT3 "150/− 20ºC", 75 cycles. D. AT5 "250/− 20ºC", 100 cycles. B and C include an inset with 30x magnification.

groups AT2 and AT3 also exhibit an optimal correlation but at a slightly lower level than AT1. It is confirmed that the data population in these groups shows a slightly larger dispersion. For AT4, AT5, and AT6, their R2 values are marginally lower than those of the previous three groups. These groups reveal two distinct clusters of values in the lower and upper regions of the linear pattern, with some values appearing significantly distant from the equation line. This confirmation supports the sensitivity of the material to the presence of microcracks between calcite grains, as indicated by [66]. The observed loss of resistance in granular materials is attributed preferentially to the coalescence of microcracks resulting from thermal behavior.

Regarding the correlation between the Non-Destructive Testing (NDT) ultrasound technique and Destructive Testing (DT) MPa values, the R2 values generally decrease compared to the previous correlation. Specifically, AT1, AT2, and AT3 exhibit valid but more discreet values (approximately 0.95), and the data dispersion and its linear approximation are less precise than in the previous cases. However, for AT4, AT5, and AT6, better linearities are observed. It is also noted that in these thermal ranges (200 to 300 ºC), there are two defined areas: one covering values between 4000 m/s and 60 MPa, and another ranging

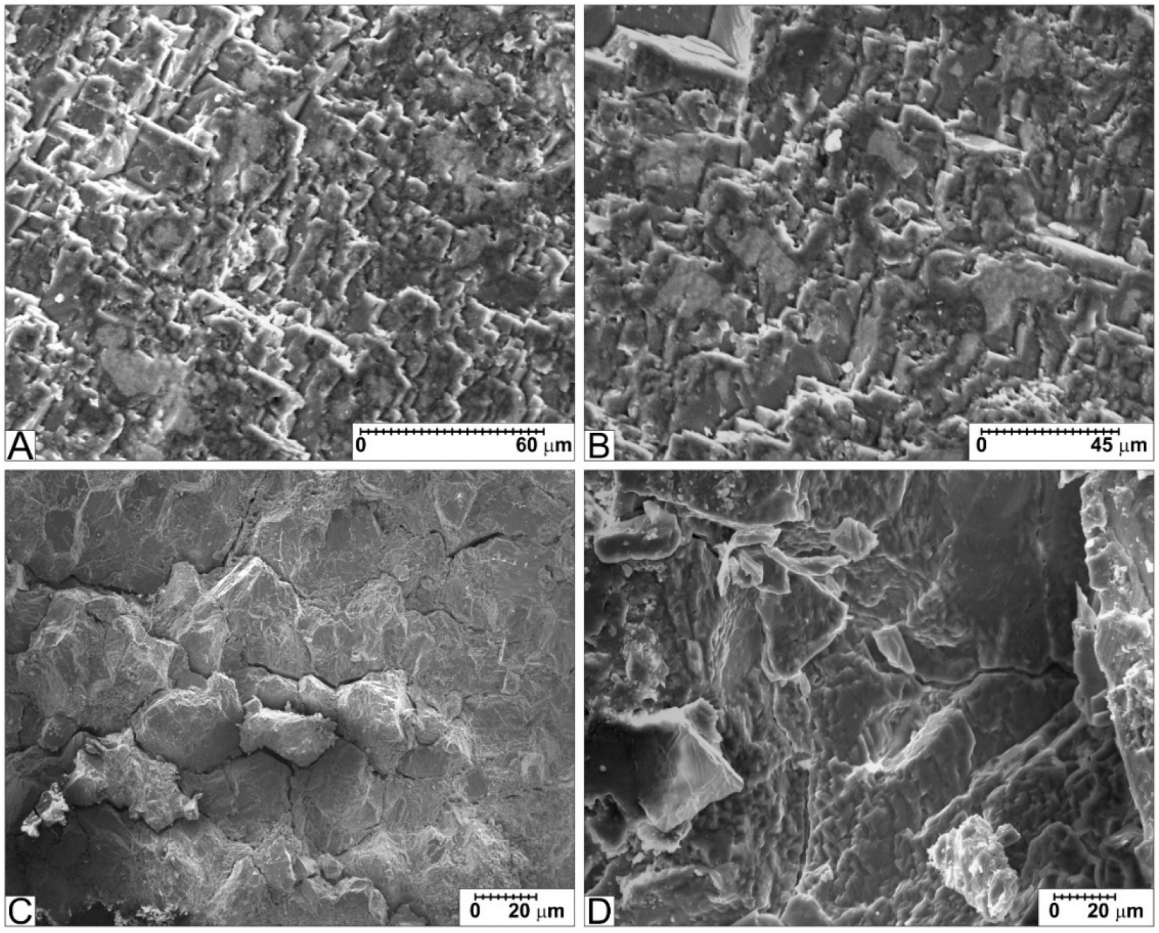

Fig. 9. Details of the samples observed using scanning electron microscopy (SEM) for different states of degradation due to thermal stress. A. AT0 "0" cycles. B. AT1 "50/− 20ºC", 25 cycles. C. AT3 "150/− 20ºC", 75 cycles. D. AT5 "250/− 20ºC", 100 cycles.

from 5000 m/s up to 70 MPa. These variations among groups are significant and may correspond to the heterogeneity within the sample.

The correlation group of cycles assessed using Non-Destructive Testing (NDT) techniques, specifically ultrasounds and rebound values, conforms more precisely to high R2 values (0.98 and 0.99). In the three initial thermal ranges, the data are consistently grouped closely to the correlation line and are well-distributed across the entire spectrum of values. However, for AT4, AT5, and AT6, despite presenting very good R2 values, there is a repeated sectorization of values in high and low areas, respectively. Nonetheless, their data align almost millimetrically with the correlation pattern.

Finally, the correlation between each non-destructive test and the destructive test was analyzed, as illustrated in Figs. 13, 14, and 15.

7.2. Correlation between Schmidt Hammer rebound and compressive strength

The correlation between rebound and compressive strength values (see Fig. 13) reveals a correlation coefficient, R2, of 0.91. This signifies a strong correlation between the two tests, consistent with findings from prior research [66–68]. Notably, a similar correlation persists even in samples subjected to up to 100 heating and cooling cycles, as demonstrated in this study. Strong correlation is also evident in the values obtained during the early stages of the test, when the most pronounced changes occurred.

The graph depicts a direct linear relationship between the results of both tests, confirming that samples with higher rebound values also exhibit higher compressive strength values. The impact of the accelerated ageing test is similarly reflected in both parameters, with reduced values observed in both tests.

7.3. Correlation between ultrasonic pulse velocity and compressive strength

In Fig. 14, the correlation (R2) between ultrasonic pulse velocity (a non-destructive test) and compressive strength (a destructive test) values for the marble samples is presented, with an R2 value of 0.92. This is nearly 1% higher than the previous correlation value, indicating greater consistency between the results of the two tests. As in the previous case, a strong correlation between the results is observed.

7.4. Correlation between ultrasonic pulse velocity and Schmidt Hammer rebound

Finally, the correlation between the two non-destructive tests, ultrasonic pulse velocity (Vp) and Schmidt Hammer rebound, was assessed, as illustrated in Fig. 15. The correlation coefficient (R2) is 0.99, indicating a strong correlation between the values obtained in the two tests. This high correlation coefficient reaffirms the consistent relationship between these two non-destructive test methods, providing a reliable combination for assessing the properties of the marble.

Upon analyzing the results, and in alignment with [698], relationships with R2 values ≥ 0.85 are considered to indicate a strong interdependence of material properties.

In this study, high correlations were found among all tests, with R2 values ranging from a minimum of 0.99 (correlation between Rebound

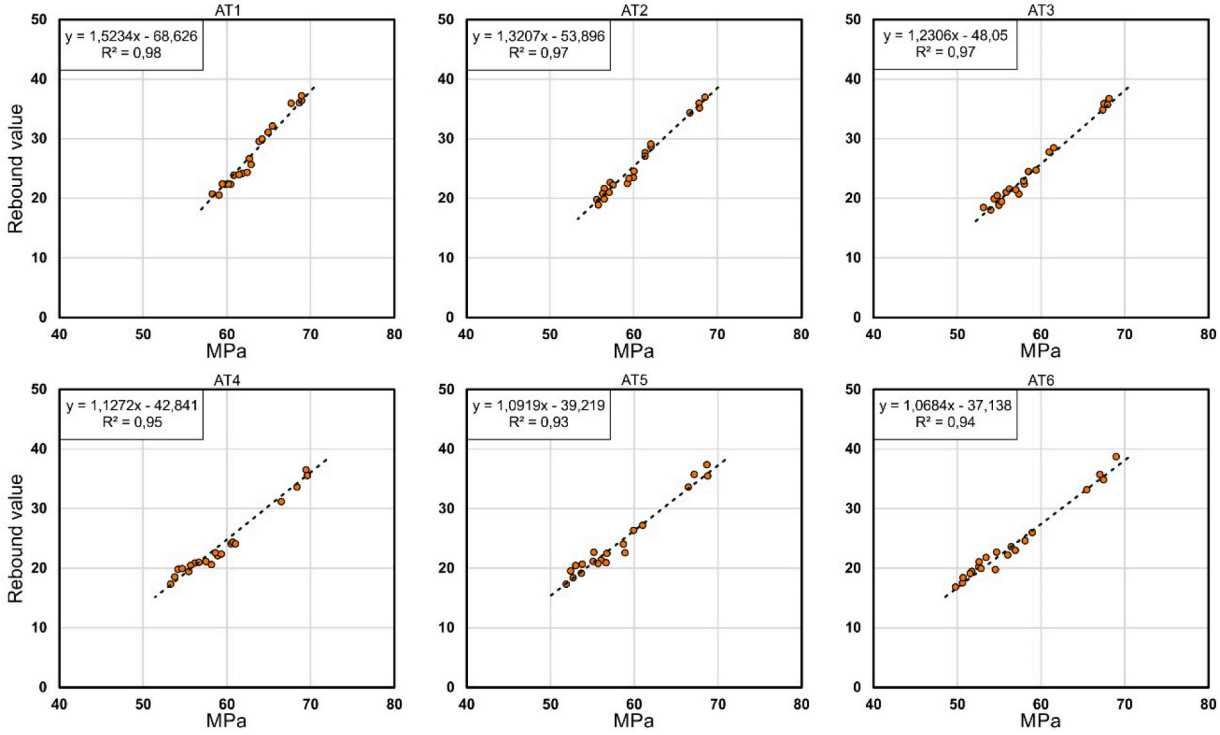

Fig. 10. Correlation for the different batch of temperature: AT1, AT2, AT3, AT4, AT5, and AT6) of Rebound values (R) versus compressive strength values (MPa) for the samples of Macael marble.

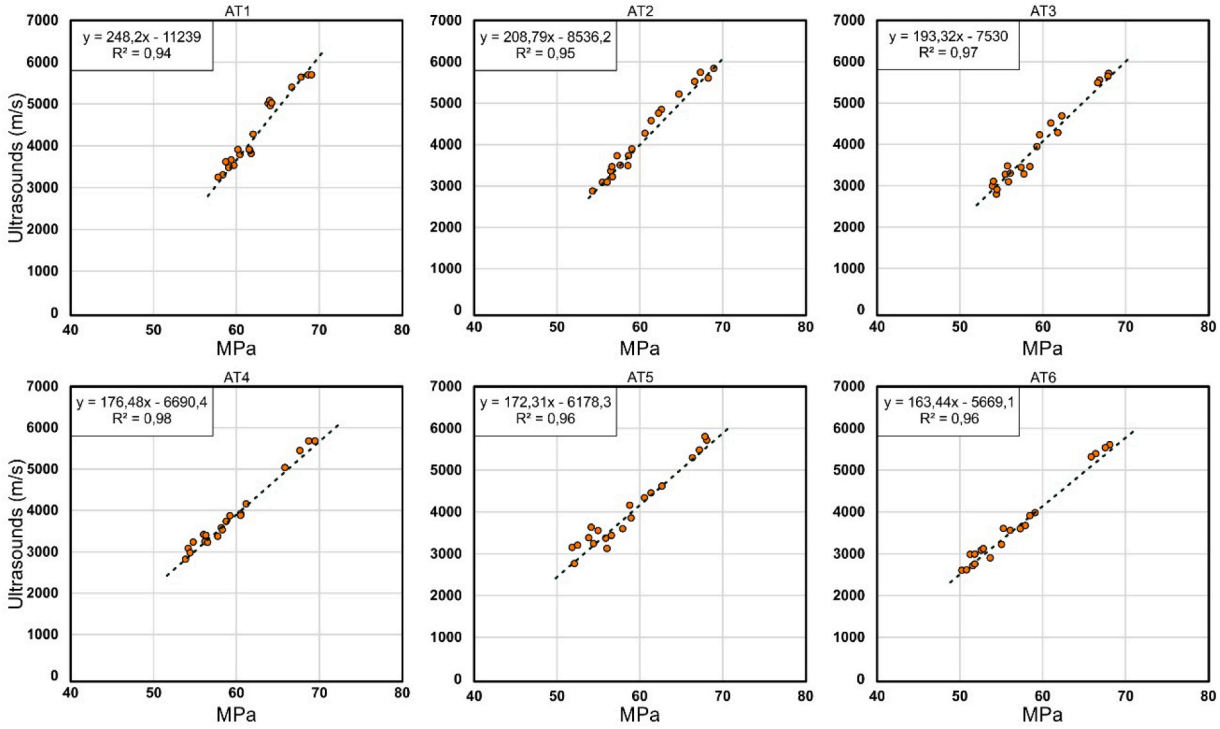

Fig. 11. Correlation for the different batch of temperature: AT1, AT2, AT3, AT4, AT5, and AT6) of ultrasonic velocity (m/s) versus compressive strength values (MPa) for the samples of Macael marble.

value and ultrasonic pulse velocity) to a maximum of 0.92 (correlation between compressive strength and Rebound value). In all cases, accelerated ageing tests resulted in a reduction of values compared to the untreated control sample.

8. Discussion

In the current investigation conducted on Macael marble, the impact of thermal weathering proves to be particularly noteworthy. As indicated by [54], the breakdown of marble within various temperature

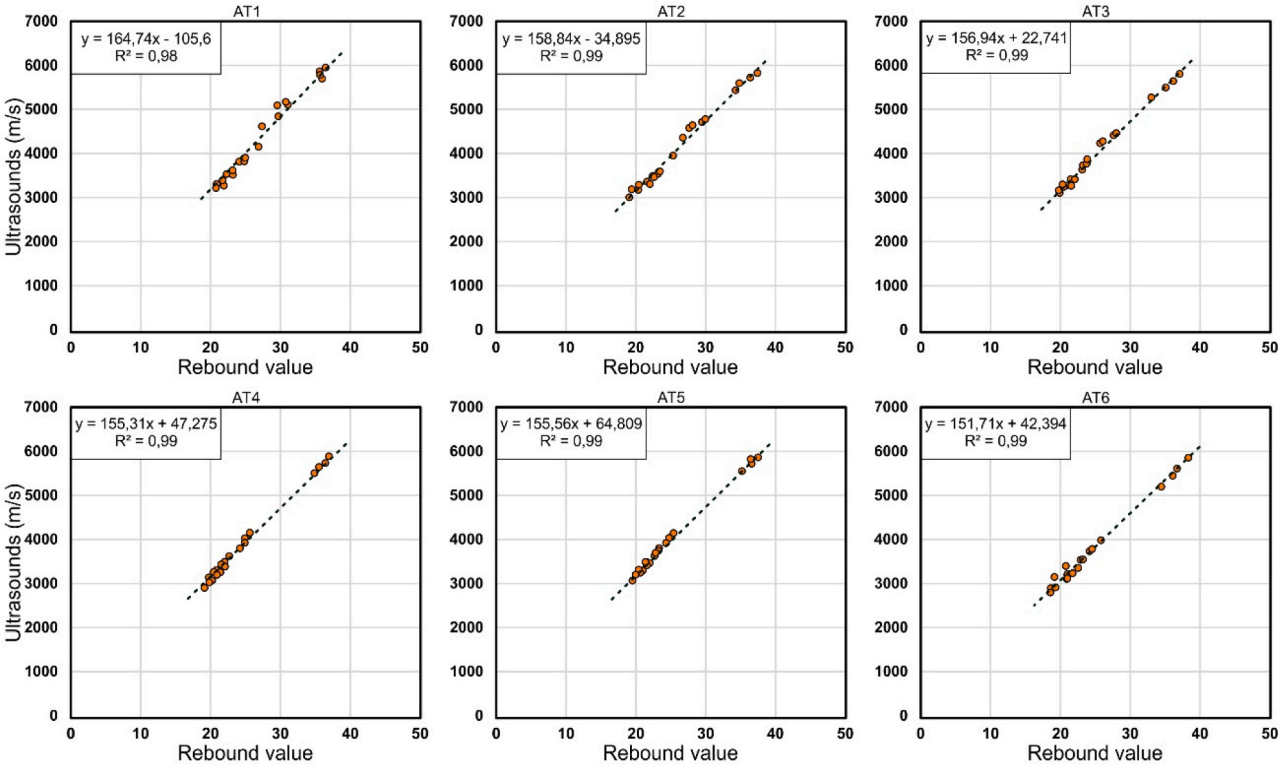

Fig. 12. Correlation for the different batch of temperature: AT1, AT2, AT3, AT4, AT5, and AT6) of Rebound values (R) versus ultrasonic velocity (m/s) for the samples of Macael marble.

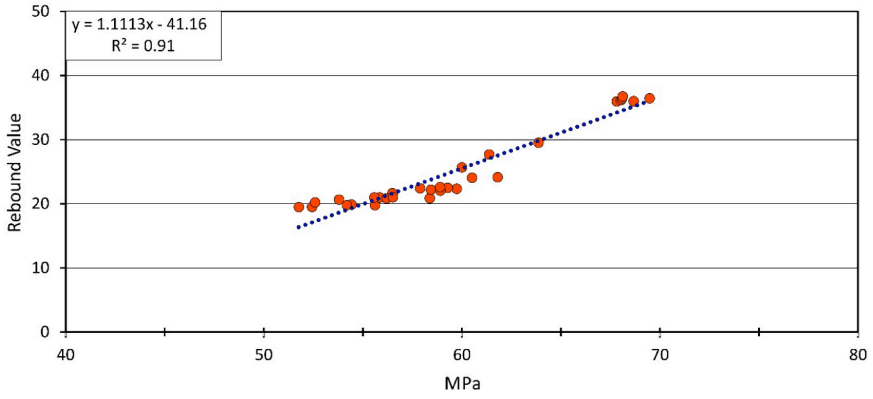

Fig. 13. Rebound values (R) versus compressive strength values (MPa) for the samples of Macael marble. Results for all the groups (AT1, AT2, AT3, AT4, AT5, and AT6).

ranges results in a notable reduction in its mechanical strength properties. The study mentioned earlier asserts that this decline in mechanical properties is intrinsic to six marble types, Macael marble included.

The most notable decreases in strength, compared to the untreated material, are noted after 100 cycles within the range of − 20/300 °C. This aligns with the discoveries outlined in [44], which proposed that the most severe weathering damage took place in marble samples heated to temperatures exceeding 200 °C after four one-hour cycles. Moreover, the obtained results affirm that, while high temperatures play a crucial role in the produced effect in absolute terms, there is also a significant impact in the lower temperature ranges, even with just 25 and 50 cycles.

Research conducted on other types of marble [43,60] has revealed that the critical temperature at which thermally induced microcracks can initiate and propagate in marble depends on various factors, including grain size and the shape of grain boundaries. For this specific type of marble, in a dry state and in accordance with [38,39,70,71–73], alterations can be observed at what is considered low temperatures (40–50 °C). In the current study, at temperatures of 300 ºC, the reduction in the speed of ultrasonic waves (Vp) and the rebound value confirm a measure of the decrease in the material's resistance capacity exceeding 46%. This decrease is associated with a state of 20 μm intergranular cracking.

The correlations established for different Non-Destructive Testing (NDT) versus Destructive Testing (DT) techniques, as well as for various groups of thermal alteration (AT1-AT6), suggest that non-destructive techniques yield the most robust and sensitive correlation results. These techniques prove to be powerful tools for evaluating the deteriorations caused in Macael marble by thermal gradients. Specifically, the variation in the speed of ultrasonic pulses proves to be highly effective in highlighting the aforementioned deteriorations.

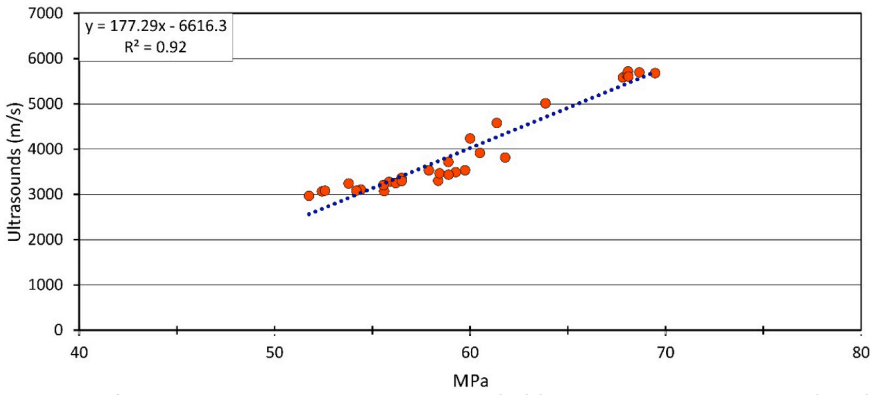

Fig. 14. Correlation between ultrasonic velocity (m/s) and compressive strength (MPa) values for the samples of Macael marble. Results for all groups (AT1, AT2, AT3, AT4, AT5, and AT6).

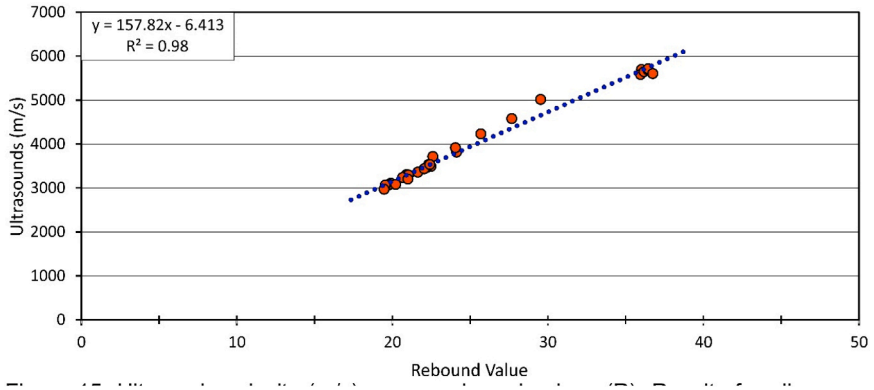

Fig. 15. Ultrasonic velocity (m/s) versus rebound values (R). Results for all groups (AT1, AT2, AT3, AT4, AT5, and AT6).

The freezing, tempering, and forced heating cycles evidently govern the degradation of Macael marble, as documented by the substantial reduction in its mechanical properties.

The test results and correlations suggest that the damage induced by the tests is associated with often imperceptible alterations and discontinuities in the marble. This indicates a heightened sensitivity of Macael marble to temperature changes, as corroborated in prior publications and studies [44,54,62]. The observed damage is attributed to the expansion and contraction of calcite crystals, which undergo significant harm when the marble is subjected to high and sustained levels of thermal stress. The detailed examination of Macael marble allows us to affirm that the decrease in mechanical properties, coupled with the increase in crystallographic deterioration, is substantial and exhibits a linear behavior. This contrasts with the findings of [54], who noted varied responses in different marble materials, highlighting the influence of petrography on each material's reaction to deterioration.

In line with [34,61], our findings affirm that the combination of the two non-destructive tests enhances the assessment of the mechanical resistance of marble. This improvement is evident as both test parameters—ultrasonic pulse speed and rebound value—demonstrate a strong correlation with compressive strength.

Moreover, as verified by [66], caution is advised against incorporating additional variables (e.g., density, porosity) when establishing empirical relationships for practical use. This precaution is taken to prevent complementarity of results that could lead to an inadequate interpretation of the reduction in mechanical resistance values.

9. Conclusions

The study's novelty and the significance of its results are underscored, given the absence of prior experiences with the study conditions applied to Macael marble and its analysis through result correlation. The application of these methods validates the use of non-destructive tests to comprehend the mechanical capacity of this material, both in its natural state and after exposure to accelerated thermal ageing cycles.

The main conclusions derived from the study confirm its advantages and are as follows:

1. The relevance of the number of cycles and the applied temperature ranges is emphasized to confirm the validation of the obtained results, underscoring the importance and novelty of experiments conducted under varying conditions. Additionally, the study highlights the observed changes in the marble and their consequences, particularly the reduction in mechanical resistance. This approach allows for determining the evolution of the mechanical behavior of the studied material
2. Furthermore, the applied temperature cycles and the results of various tests reveal a direct relationship between the temperature gradient and the loss of mechanical properties in Macael marble. The increase in thermal gradient has a significant impact, leading to a progressive decrease in values and, consequently, qualities compared to the material not subjected to any gradient. This loss is attributed to the modification of the intergranular state and the separation of boundaries due to thermal expansion [52,53,69].
3. The results obtained from optical microscopy and scanning electron microscopy analysis underscore how successive expansions and contractions, resulting from ageing cycles, lead to irreversible intergranular and intra-granular spaces. This factor implies a loss of mechanical cohesion and an increase in the porosity of the stone

material. Acquiring this knowledge enables the establishment of protective measures for construction elements.
4. The correlation system provides a precise understanding of the material's behavior when analyzed through various techniques applied to a material subjected to significant cycles with intentionally increased thermal environmental conditions. In this study, the high correlation coefficient (R2) confirms the utility of non-destructive techniques (NDT) in evaluating the behavior of this type of marble.
5. The study recognizes the capability to assess deterioration in white Macael marble and similar materials through the correlation of non-destructive tests.
6. Utilizing non-destructive testing (NDT) to assess deterioration in heritage sites reduces costs and ensures monument preservation, providing crucial information for heritage management.

Future studies will increase the number of cycles to better understand the material's deterioration progression and observe it at a macroscopic scale.

CRediT authorship contribution statement

Durán-Suárez Jorge: Writing – review & editing, Writing – original draft, Visualization, Validation, Supervision, Resources, Project administration, Methodology, Investigation, Funding acquisition, Formal analysis, Data curation, Conceptualization. **Castro-Gomes Joao:** Writing – original draft, Visualization, Validation, Supervision, Resources, Methodology, Investigation. **SÁEZ-PÉREZ MARIA PAZ:** Writing – review & editing, Writing – original draft, Visualization, Validation, Supervision, Resources, Project administration, Methodology, Investigation, Formal analysis, Data curation, Conceptualization.

Declaration of Competing Interest

The authors declare that they have no known competing financial interests or personal relationships that could have appeared to influence the work reported in this paper.

Data Availability

Data will be made available on request.

Acknowledgements

This research was funded by Pre-competitive Research Projects Program, belonging to the Research and Transfer Plan of the University of Granada (PP2022. PP.27) and was supported by the REMINE Project Programme for Research and Innovation Horizon 2020 Marie Skłodowska-Curie Actions, Horizon 2020, WARMEST Project Research and Innovation Staff Exchange (RISE) H2020-MSCA-RISE-2017, RRRMaker project Marie Skłodowska-Curie Research and Innovation Staff Exchange, and Scientific Unit of excellence "Ciencia en la Alhambra," ref. UCE-PP2018-01 (University of Granada) and was carried out under the auspices of Research Group RNM 0179 and HUM 629 of the Junta de Andalucía.

References

[1] T. Theocharis Katrakazis, A. Heritage, C. Dillon, P. Juvan, S. Golfomitsou, Enhancing research impact in heritage conservation, Stud. Conserv. 63 (8) (2018) 450–465, https://doi.org/10.1080/00393630.2018.1491719.
[2] T. Huynh, B.-P. Nguyen, A.M.S. Pradhan, Q.-Q. Pham, Vision-based inspection of bolted joints: field evaluation on a historical truss bridge in Viet Nam, Vietnam. J. Mech. 36 (77) (2020), https://doi.org/10.15625/0866-7136/15073.
[3] F. Rodrigues, R. Matos, M. Di, A. Costa, Conservation level of residential buildings: methodology evolution, Constr. Build. Mater. 172 (2018) 781–786, https://doi.org/10.1016/j.conbuildmat.2018.03.129.
[4] G. Ruggiero, R. Marmo, M. Nicolella, A methodological approach for assessing the safety of historic buildings' façades, Sustainability 13 (2021) 2812, https://doi.org/10.3390/su13052812.
[5] Chaves Moreno, E.A.; Pachón García, P.; Cámara Pérez, M.; Compán Cardiel, V. Caracterización de propiedades dinámicas de edificios patrimoniales mediante análisis modal operacional. V Congreso Internacional sobre documentación, conservación y reutilización del patrimonio arquitectónico y paisajístico. Granada. 18 al 21 de octubre de 2017.
[6] G. Mardones, The defense of the architectural heritage. The chilean case, ARQUITEXTOS 25 (33) (2018) 73–86.
[7] J. Rey Rey, P. Vegas González, J. Ruiz Carmona, Structural refurbishment strategies for industrial heritage buildings in Madrid: Recent examples, Hormig. Y. Acero 69 (285) (2018) 91–99, https://doi.org/10.1016/j.hya.2018.05.001.
[8] A.Z. Sampaio, A.M. Pinto, A.M. Gomes, A. Sanchez-Lite, Generation of an HBIM library regarding a palace of the 19th century in Lisbon, Appl. Sci. 11 (2021) 7020, https://doi.org/10.3390/app11157020.
[9] B. Onecha, A. Dotor, C. Marmolejo-Duarte, Beyond cultural and historic values, sustainability as a new kind of value for historic buildings, Sustainability 13 (2021) 8248, https://doi.org/10.3390/su13158248.
[10] Salman, M., Hmood, K.2019). Conservation of Historic Districts: Challenges of Integration in Modern Cities within Sustainable Perspective. In XIII CTV 2019 Proceedings: XIII International Conference on Virtual City and Territory: "Challenges and paradigms of the contemporary city": UPC, Barcelona, October 2–4, 2019. Barcelona: CPSV, 2019, p. 8530. E-ISSN 2604–6512. https://dx.doi.org/10.5821/ctv.8530.
[11] ⟨https://es.unesco.org/sdgs⟩.
[12] J. Hosagrahar, Culture at the heart of the SDGs, UNESCO Cour. 1 (2017) 12–14. ⟨https://es.unesco.org/courier/april-june-2017/cultura-elemento-central-ods⟩.
[13] ⟨https://eur-lex.europa.eu/legal-content/ES/TXT/HTML/?uri=CELEX:52019DC0022&from=PT⟩.
[14] A. Borri, M. Corradi, Architectural heritage: a discussion on conservation and safety, Heritage 2 (2019) 631–647, https://doi.org/10.3390/heritage2010041.
[15] F. Du, K. Okazaki, C. Ochiai, H. Kobayashi, Post-disaster building repair and retrofit in a disaster-prone historical village in China: A case study in Shangli, Sichuan, Int. J. Disaster Risk Reduct. 16 (2016) 142–157, https://doi.org/10.1016/j.ijdrr.2016.02.007.
[16] J. Yi, W. Park, S. Lee, T. Huynh, J. Kim, C. Seo, Evaluation of vibration characteristics of an existing harbor caisson structure using tugboat impact tests and modal analysis, Int. J. Ofdistributed Sens. Netw. 2013 (1–11) (2013), https://doi.org/10.1155/2013/806482.
[17] J.-P. Balayssac, V. Garnier, Non-Destructive Testing and Evaluation of Civil Engineering Structures; Elsevier. Science, Amsterdam, The Netherlands, 2017. ISBN 9780081023051.
[18] G. Ramesh, D. Srinath, D. Ramya, B. Vamshi Krishna, Repair, rehabilitation and retrofitting of reinforced concrete structures by using non-destructive testing methods (in press.), Mater. Today Proc. (2021), https://doi.org/10.1016/j.matpr.2021.02.778.
[19] B. Nowogónska, Consequences of abandoning renovation: case study—neglected industrial heritage building, Sustainability 12 (2020) 6441, https://doi.org/10.3390/su12166441.
[20] Ł. Drobiec, K. Grzyb, J. Zaja_c, Analysis of reasons for the structural collapse of historic buildings, Sustainability 13 (2021) 10058, https://doi.org/10.3390/su131810058.
[21] B. Menéndez, Non-destructive techniques applied to monumental stone conservation, Non-Destr. Test. Chapter 8 (2016) 169–209, https://doi.org/10.5772/62408.
[22] J.R. Deepak, V.K.B. Raja, D. Srikanth, H. Surendran, M.M. Nickolas, Non-destructive testing (NDT) techniques for low carbon steel welded joints: A review and experimental study, Mater. Today Proc. 44 (2021) 3732–3737, https://doi.org/10.1016/j.matpr.2020.11.578.
[23] Diaferio, M. Correlation Curves for Concrete Strength Assessment Through Non-Destructive Tests. ⟨https://doi.org/10.2139/ssrn.4177623⟩.
[24] A. Tavukçuoğlu, Non-destructive testing for building diagnostics and monitoring: experience achieved with case studies, 2nd International Congress on Materials & Structural Stability (CMSS-2017), MATEC Web Conf. 149 (2018) 01015, https://doi.org/10.1051/matecconf/201814901015.
[25] K. Grzyb, Ł. Drobiec, J. Blazy, J. Zaja_c, The use of NDT diagnostic methods and calculations in assessing the masonry tower crowned with the steel dome, Materials 15 (2022) 7196, https://doi.org/10.3390/ma15207196.
[26] P.B. Lourenço, Conservation of cultural heritage buildings: methodology and application to case studies, Rev. ALCONPAT 3 (2) (2013) 98–110, https://doi.org/10.21041/ra.v3i2.46.
[27] B. Tejedor, E. Lucchi, D. Bienvenido-Huertas, I. Nardi, Non-destructive techniques (NDT) for the diagnosis of heritage buildings: Traditional procedures and futures perspectives, Energy Build. 263 (2022) 112029, https://doi.org/10.1016/j.enbuild.2022.112029.
[28] M. Umzarulazijo Umar, M. Hanizun Hanafi, N. Abdul Latip, Analysis of non-destructive testing of historic building structures, Aust. J. Basic Appl. Sci. 9 (7) (2015) 326–330. ISSN:1991-8178.
[29] Yasser El Masri, Tarek Rakha, A scoping review of non-destructive testing (NDT) techniques in building performance diagnostic inspections, 120542, Constr. Build. Mater. 265 (2020) 30, https://doi.org/10.1016/j.conbuildmat.2020.120542.
[30] M. Bramanti, E. Bozzi, An ultrasound based technique for the detection and classification of flaws inside large sizes marble or stone structural elements, Int. Cult. Herit. Inform. Meet. (2001) 283–287.

[31] B. Kouddane, Z.M. Sbartaï, M. Alwash, K. Ali-Benyahia, S.M. Elachachi, N. Lamdouar, S. Kenai, Assessment of concrete strength using the combination of ndt—review and performance analysis, Appl. Sci. 12 (2022) 12190, https://doi.org/10.3390/app122312190.
[32] Samson, D., Tope Moses, O. Correlation between Non-Destructive Testing (NDT) and Destructive Testing (DT) of Compressive Strength of Concrete. International Journal of Engineering Science Invention, 2014, 3, 9, pp.12–17ISSN (Online): 2319 – 6734, ISSN (Print): 2319 – 6726.
[33] Theodoridou, M., Dagrain, F., Ioannou, I. Correlation of stone properties using standardized methodologies and non-standardized micro-destructive techniques. 12th International Congress on the Deterioration and Conservation of Stone Columbia University, New York, 2012.
[34] R. Fort, J. Feijoo, M.J. Varas–Muriel, M.A. Navacerrada, M.M. Barbero-Barrera, D. De la Prida, Appraisal of non-destructive in situ techniques to determine moisture- and salt crystallization-induced damage in dolostones, J. Build. Eng. 53 (2022) 104525.
[35] G. Forestieri, A. Tedesco, M. Ponte, The stone in a monumental masonry building of the Tyrrhenian coast (Italy): new data on the relationship between stone properties and structural analysis, GE-Conserv. 11 (2017) 102–109.
[36] Marijana Hadzima-Nyarko Hrvoje Glavaš, Ivana Haničar Buljan, Tomislav Barić. Locating, Hidden elements in walls of cultural heritage buildings by using infrared thermography, Buildings 9 (2019) 32, https://doi.org/10.3390/buildings90200.
[37] R. Fort, M.J. Varas, M. Alvarez de Buergo, D. Martin-Freire, Determination of anisotropy to enhance the durability of natural stone, IOP Publ. J. Geophys. Eng. 8 (2011) S132–S144, https://doi.org/10.1088/1742-2132/8/3/S13.
[38] S. Battaglia, M. Franzini, F. Mango, High-sensitivity apparatus for measuring linear thermal expansion: Preliminary results on the response of marbles to thermal cycles, Il Nuovo Cim. 16 (4) (1993) 453–461, https://doi.org/10.1007/BF02507653.
[39] K. Malaga-Starzec, J.E. Lindqvist, B. Schouenborg, Experimental study on the variation in porosity of marble as a function of temperature, Geol. Soc. Spec. Publ. 205 (2002) 81–88, https://doi.org/10.1144/GSL.SP.2002.205.01.07.
[40] V. Shushakova, E.R. Fuller Jr, F. Heidelbach, D. Mainprice, S. Siegesmund, Marble decay induced by thermal strains: simulations and experiments, Environ. Earth Sci. 69 (2013) 1281–1297, https://doi.org/10.1007/s12665-013-2406-z.
[41] A. Murru, D.M. Freire-Lista, R. Fort, M.J. Varas-Muriel, P. Meloni, Evaluation of post-thermal shock effects in Carrara marble and Santa Caterina di Pittinuri limestone, Constr. Build. Mater. 186 (2018) 1200–1211, https://doi.org/10.1016/j.conbuildmat.2018.08.034.
[42] S. Siegesmund, T. Weiss, E.K. Tschegg, Control of marble weathering by thermal expansion and rock fabrics, Proc. 9th Int. Congr. Deterioration Conserv. Stone (2000) 205–213, https://doi.org/10.1016/b978-044450517-0/50102-1.
[43] Siegfried Siegesmund, H. Dürrast, Physical and mechanical properties of rocks, in: Siegesmund Siegfried, R. Snethlage (Eds.), Stone in Architecture: Properties, Durability, 4th ed..,, Springer, 2011, pp. 97–225, https://doi.org/DOI10.1007/978-3-642-14475-2_3.
[44] A. Ahmad, Investigation of marble deterioration and development of a classification system for condition assessment using non-destructive ultrasonic technique, Mediterr. Archaeol. Archaeom. Vol. 20 (No 3) (2020) 75–89, 2020.
[45] G.F. Andriani, L. Germinario, Thermal decay of carbonate dimension stones: fabric, physical and mechanical changes, Environ. Earth Sci. 72 (2014) 2523–2539, https://doi.org/10.1007/s12665-014-3160-6.
[46] El Boudani, M. Wilkie-Chancellier, N. Martinez, L. Hébert, R. Rolland, O. Forst, S. Vergès-Belmin, V. Serfaty, Marble Characterization by ultrasonic methods, S (2015), https://doi.org/10.1016/j.proeps.2015.08.061.
[47] J. Rodríguez-Gordillo, M.P. y Sáez-Pérez, Effects of thermal changes on Macael marble: experimental study, Constr. Build. Mater. 20 (2006) 355–365, https://doi.org/10.1016/j.conbuildmat.2005.01.061.
[48] R. Bellopede, E. Castelletto, B. Schouenborg, P. Marini, Assessment of the European standard for the determination of resistance of marble to thermal and moisture cycles: recommendations for improvements, Environ. Earth Sci. 75 (2016) 946. DOI 10.1007/s12665-016-5748-5.
[49] E. Franzoni, E. Sassoni, G.W. Scherer, S. Naidu, Artificial weathering of stone by heating, J. Cult. Herit. 14 (3 SUPPL) (2013) e85–e93, https://doi.org/10.1016/j.culher.2012.11.026.
[50] J. Ruedrich, C. Knell, J. Enseleit, Y. Rieffel, S. Siegesmund, Stability assessment of marble statuaries of the Schlossbru (Berlin, Germany) based on rock strength measurements and ultrasonic wave velocities, Environ. Earth Sci. 69 (2013) 1451–1469, https://doi.org/10.1007/s12665-013-2246-x.
[51] Johanna Menningen, Siegfried Siegesmund, Daryl Tweeton, Markus Träupmann, Ultrasonic tomography:non-destructiv evaluation of the weathering state on a marble obelisk, considering the effect of structural properties, Environ. Earth Sci. 77 (2018), https://doi.org/10.1007/s12665-018-7776-9.
[52] J. y Rodríguez-Gordillo, M.P. Sáez Pérez, Comportamiento físico del mármol blanco de Macael (España) por oscilación térmica de bajo y medio rango, Mater. De. Constr. 60 (297) (2010) 127–141, https://doi.org/1.3989/mc.2010.44107.
[53] M.P. Sáez-Pérez, J. y Rodríguez-Gordillo, Structural and compositional anisotropy in Macael marble (Spain) by ultrasonic, XRD and optical microscopy methods, Constr. Build. Mater. 23 (6) (2009) 2121–2126, https://doi.org/10.1016/j.conbuildmat.2008.10.013.
[54] S. Siegemund, J. Menningen, V. Shushakova, Marble decay: towards a measure of marble degradation based on ultrasonic wave velocities and thermal expansion data, Environ. Earth Sci. 80 (2021) 395, https://doi.org/10.1007/s12665-021-09654-y.
[55] R. Navarro, D. Pereira, A.S. Cruz, G. Carrillo, The significance of whitemacael marble since ancient times: characteristics of a candidate as global heritage stone resource, Geoheritage 11 (2019) 113–123, https://doi.org/10.1007/s12371-017-0264-x.
[56] C.G. Egeler, On the tectonics of the eastern Betic Cordilleras, Geol. Rundsch., LIII (1963) 260–269.
[57] R. Navarro, A. Cruz, L. Arriaga, J.M. y Baltuille, Caracterización de los principales tipos de mármol extraídos en la comarca de Macael (Almería, sureste de España) y su importancia a lo largo de la historia, Bol. Geológico Y. Min. 128 (2) (2017) 345–361, https://doi.org/10.21701/bolgeomin.128.2.005.
[58] A.C. Martín-Algarra, F.M. Alonso-Chaves, B. Andreo, J.M. Azañón, J.C. Balanyá, G. Booth-Rea, A. Crespo-Blanc, F. Delgado, A. Díaz de Federico, A. Estévez, J. Galindo-Zaldívar, A. García-Casco, V. García-Dueñas, C.J. Garrido, F. Gervilla, F. González-Lodeiro, A. Jabaloy, A.C. López-Garrido, A. Martín-Algarra, M. Martín-Martín, J.M. Nieto, L. O'Dogherty, M. Orozco, E. Puga, R. Rodríguez-Cañero, M. D. Ruiz-Cruz, A. Sánchez-Gómez, A. Sánchez-Navas, C. Sanz de Galdeano, J.I. Soto, R.L. Torres-Roldán, J.A. y Vera, Zonas Internas Béticas, in: J.A. En: Vera (Ed.), Geología de España, SGE-IGME, Madrid, 2004, pp. 395–444.
[59] Sáez-Pérez, M.P. 2004. Estudio de elementos arquitectónicos y composición de materiales del Patio de los Leones. Interacciones en sus causas de deterioro. Servicio de publicaciones de la Universidad de Granada, Granada, 429 pp.
[60] D.L. Whitney, B.W. Evans, Abbreviations for names of rock-forming minerals, Am. Mineral. 95 (2010) (2010) 185–187, https://doi.org/10.2138/am.2010.3371.
[61] M.P. y Sáez-Pérez, J. Rodríguez-Gordillo, The influence of solar radiation on the deterioration of the marble columns in the courtyard of the lions in the alhambra, Stud. Conserv. 53 (3) (2008) 145–157, https://doi.org/10.2307/27867034.
[62] K. Laskaridis, A. Arapakou, M. Patronis, I. Kouseris, Correlations between the physical mechanical properties of Greek dimension stones, Mater. Proc. 5 (2021) 28, https://doi.org/10.3390/materproc2021005028.
[63] ASTM D 5873–00 Standard Test Method for Determination of Rock Hardness by Rebound Hammer Method; ASTM Stand. International: West Conshohocken, PA, USA, 2001.
[64] Non-destructive testing-Ultrasonic testing-Transmission technique (ISO 16823: 2012).
[65] UNE-EN 1926:2007Natural stone test methods - Determination of uniaxial compressive strength.
[66] A. Aydin, A. Basu, The Schmidt hammer in rock material characterization, Eng. Geol. 81 (2005) 1–14, https://doi.org/10.1016/j.enggeo.2005.06.006.
[67] Ciornei N., Cetean, V., Facaoaru, I. Non-destructive method for rapid "in situ" characterization of rocks, 2004. Bulletin of the Geologicl Society of Greece, 2004, vol. XXXVI. Proceedings of the 10th International Congress, Thessaloniki, Greece.
[68] R. Fort, M. Alvarez de Buergo, E.M. Perez-Monserrat, Non-destructive testing for the assessment of granite decay in heritage structures compared to quarry Stone, Int. J. Rock. Mech. Min. Sci. 61 (2013) 296–305, https://doi.org/10.1016/j.ijrmms.2012.12.048.
[69] H. Aldeeky, O. Al Hattamleh, S. Rababah, Assessing the uniaxial compressive strength and tangent Young's modulus of basalt rock using the Leeb rebound hardness test, Mater. De. Constr. 70 (340) (2020) e230, https://doi.org/10.3989/mc.2020.15119.
[70] T. Weiss, S. Siegesmund, E.R. Fuller Jr ., Thermal stresses and microcracking in calcite and dolomite marbles via finite element modelling, in: S. Siegesmund, T. Weiss, A. Vollbrecht (Eds.), Natural Stone, Weathering Phenomena, Conservation Strategies and Case Studies, 2002, pp. 89–102.
[71] M. Steiger, A.E. Charola, K. Sterflinger, Weathering and deterioration, in: Siegfried Siegesmund, R. Snethlage (Eds.), Stone in Architecture: Properties, Durability (4th ed., Springer, 2011, pp. 227–316, https://doi.org/DOI 10.1007/978-3-642-14475-2_5.
[72] C. Widhalm, E. Tschegg, W. Eppensteiner, Acoustic emission and anisotropic expansion when heating marble, J. Perform. Constr. Facil. 11 (1) (1997) 35–40, https://doi.org/10.1061/(ASCE)0887-3828(1997)11:1(35).
[73] D. Benavente, J. Martinez-Martinez, J.J. Galiana-Merino, C. Pla, M. de Jongh, N. Garcia-Martinez, Estimation of uniaxial compressive strength and intrinsic permeability from ultrasounds in sedimentary stones used as heritage building materials, J. Cult. Herit. 55 (2022) 346–355, https://doi.org/10.1016/j.culher.2022.04.010.